Published in final edited form as:

Nat Plants. ; 2: 16025. doi:10.1038/nplants.2016.25.

Local auxin metabolism regulates environment-induced hypocotyl elongation

Zuyu Zheng[1], **Yongxia Guo**[2], **Ondřej Novák**[3,4], **William Chen**[5], **Karin Ljung**[3], **Joseph P. Noel**[6,*], and **Joanne Chory**[1,*]

[1]Howard Hughes Medical Institute and Plant Biology Laboratory, The Salk Institute for Biological Studies, La Jolla, California 92037, USA

[2]The Jack H. Skirball Center for Chemical Biology and Proteomics, The Salk Institute for Biological Studies, La Jolla, California 92037, USA

[3]Umeå Plant Science Centre, Department of Forest Genetics and Plant Physiology, Swedish University of Agricultural Sciences, SE-901 83 Umeå, Sweden

[4]Laboratory of Growth Regulators, Faculty of Science, Palacký University and Institute of Experimental Botany ASCR, Šlechtielů 11, 783 71 Olomouc, Czech Republic

[5]Plant Biology Laboratory, The Salk Institute for Biological Studies, La Jolla, California 92037, USA

[6]Howard Hughes Medical Institute and The Jack H. Skirball Center for Chemical Biology and Proteomics, The Salk Institute for Biological Studies, La Jolla, California 92037, USA, Czech Republic

Abstract

A hallmark of plants is their adaptability of size and form in response to widely fluctuating environments. The metabolism and redistribution of the phytohormone auxin play pivotal roles in establishing active auxin gradients and resulting cellular differentiation. In *Arabidopsis thaliana*, cotyledons and leaves synthesize indole-3-acetic acid (IAA) from tryptophan through indole-3-pyruvic acid (3-IPA) in response to vegetational shade. This newly synthesized auxin moves to the hypocotyl where it induces elongation of hypocotyl cells. Here we show that loss of function of *VAS2* (IAA-amido synthetase Gretchen Hagen 3 (GH3).17) leads to increases in free IAA at the expense of IAA-Glu (IAA-glutamate) in the hypocotyl epidermis. This active IAA elicits shade- and high temperature-induced hypocotyl elongation largely independently of 3-IPA-mediated IAA biosynthesis in cotyledons. Our results reveal an unexpected capacity of local auxin metabolism to

*Correspondence and requests for materials should be addressed to J.P.N. and J.C. ; Email: chory@salk.edu; ; Email: noel@salk.edu

Author contributions

Z.Y.Z. designed the experiments with the input from J.P.N. and J.C., Z.Y.Z., Y.X.G., O.N., W.C. and K.L. performed the experiments. Z.Y.Z., J.P.N. and J.C. wrote the manuscript. All authors discussed the results and commented on the experimental design.

Supplementary information is available online.

Competing interests

The authors declare no competing financial interests.

modulate the homeostasis and spatial distribution of free auxin in specialized organs such as hypocotyls in response to shade and high temperature.

Plants are rooted in the ground, and, as such, rapid adaptation to suboptimal growth environments is a matter of survival. Although the number of biotic and abiotic environmental stressors is high, plants appear to utilize a small number of signalling and metabolic pathways to adapt to these stressors. For instance, *Arabidopsis* seedlings have the same phenotypic response to shade light and high temperature. In both cases, *Arabidopsis* plants elongate stems, leaves and petioles, increase leaf hyponasty and apical dominance, accelerate flowering and produce fewer seeds of low quality with substantially reduced germination efficiency[1–4]. Under shade, these responses are collectively termed the shade avoidance syndrome (SAS). SAS allows sun-loving plants to outgrow their neighbours to effectively compete for sunlight; under high temperature, these same responses are likely to promote transpiration and eventually reduced leaf temperatures[5].

The phytohormone auxin plays a prominent role in regulating both shade- and high temperature-triggered changes in seedling architecture. Shade or high temperature boosts the level of free IAA (the major natural auxin) by eliciting the dominant two-step IAA biosynthetic pathway, from tryptophan (Trp) to 3-IPA catalysed by the tryptophan aminotransferase TAA1 (Tryptophan Aminotransferase of *Arabidopsis*; also known as SAV3–TIR2–WEI8), followed by oxidative decarboxylation of 3-IPA to IAA catalysed by flavin monooxygenases in the YUCCA (YUC) subfamily[3–9]. The auxin biosynthetic mutant *sav3* (shade avoidance deficient 3) fails to rapidly produce IAA in response to shade or high temperature, thus retarding full elongation of its hypocotyl under shade or high-temperature treatment[4,6,10]. Using auxin responsive promoters fused to histochemical markers to image the spatial and temporal patterning of newly synthesized auxin, shade-induced IAA accumulates predominantly in the margins of cotyledons and young primary leaves[4]. Together with other studies documenting a requirement for auxin transport in shade-regulated hypocotyl elongation[8,11], the current model for shade-induced growth is that newly synthesized auxin arises in the cotyledons, is then transported to the hypocotyl and localizes in hypocotyl epidermal cells where it stimulates hypocotyl elongation[4,8,12]. This model may also account for high temperature-induced auxin biosynthesis and transport resulting in hypocotyl elongation[5]; however, experimental evidence for the latter chemotype and phenotype remains to be experimentally verified.

Here, we report the characterization of *VAS2* (*vas* stands for *reversal of sav*), whose loss-of-function alleles have higher levels of free and active IAA than wild-type (WT) plants even in the *sav3* mutant background with greatly attenuated IAA biosynthesis. *vas2* mutants have long hypocotyls under normal growth conditions, and rescue the short hypocotyl phenotype of *sav3* mutants in the presence of shade or high temperature. Moreover, hypocotyl elongation of *vas2* mutants is less sensitive to the inhibitory effects of auxin transport inhibitors than WT. We show that *VAS2* encodes GH3.17, an IAA-amido synthetase gene expressed predominantly in hypocotyls. We propose that local auxin metabolism in the hypocotyl plays a critical role in modulating the homeostasis, spatial distribution and

concentration gradient of unmodified and active IAA, thereby making the hypocotyl an IAA 'sink' responsive to auxin synthesized in cotyledons.

Results

Identification and characterization of *VAS2* gene and its mutants

The details for screening *sav3-1* suppressors—second-site mutations that allowed *sav3* mutants to elongate their hypocotyls in response to shade—have been described previously[13]. One suppressor, *vas2-1*, fully rescued the short hypocotyl of *sav3-1* under shade light (Fig. 1a–c). Moreover, compared with *A. thaliana* Col WT plants, *vas2-1* had longer hypocotyls under both continuous white light (Wc) and shade conditions (Fig. 1a,c).

The *vas2-1* mutation was recessive. We identified the causative mutation to be a nonsense mutation (Arg46 to stop codon) in *At1g28130* by map-based cloning (Fig. 1b). The identity of VAS2 was confirmed as follows: (1) expression of full-length *At1g28130* genomic DNA driven by its native promoter shortened the hypocotyls of *vas2-1 sav3-1* double mutants (Supplementary Fig. 1); (2) *vas2-2*, the transfer (T)-DNA knockout mutant of *At1g28130*, fully suppressed *sav3-1* short hypocotyl phenotype, and had similar phenotypes to *vas2-1* (Fig. 1a–c); and (3), *vas2-2* also rescued the short hypocotyl of the stronger *sav3* mutant allele, *sav3-3* (Fig. 1d and Supplementary Fig. 2a).

VAS2 (*At1g28130*) encodes GH3.17 (ref. [14]), a member of the eight predicted IAA-amido synthetases in *A. thaliana* that conjugate the carboxyl group of IAA to amino acids, forming inactive amide-linked auxin for storage or degradation[15–18]. Except for VAS2/ GH3.17 and GH3.9, expression of the other five IAA-amido synthetases is rapidly induced by external auxin treatment[19]. Accumulation of IAA-amido synthetases with exogenously applied IAA has been proposed as a mechanism to prevent overaccumulation of active IAA (refs [17,18,20]). In addition, phylogenetic analyses suggest that GH3.9 is the closest paralogue of VAS2[15,21]; yet, unlike *vas2*, the *gh3.9* mutant failed to suppress *sav3-3* phenotypes (Fig. 1d and Supplementary Fig. 2b). Thus, even though these IAA-amido synthetases exhibit partially overlapping enzyme activities *in vitro*[15,16], our genetic results strongly indicate that their functions are not simply redundant *in vivo*.

Disruption of *VAS2–GH3.17* increases the levels of free IAA and its biosynthetic precursors, and decreases the level of IAA-Glu. As suggested before[15], VAS2–GH3.17 is an active IAA-amido synthetase with Glu as the most efficient cosubstrate (Fig. 1e). This prompted us to quantify the levels of IAA and its anabolic and catabolic metabolites including 3-IPA, oxidized IAA (2-oxoindole-3-acetic acid, oxIAA), and the two most abundant IAA-amino acid conjugates in *Arabidopsis*, IAA-Glu and IAA-aspartate (IAA-Asp) (Fig. 2a–h)[22,23]. Both IAA-Glu and IAA-Asp are believed to lead to IAA degradation in *Arabidopsis*, since they are resistant to cleavage and release of free IAA by amidohydrolases[17,24–26]. Using the shoots of seedlings, including cotyledons, leaves and hypocotyls for quantitative measurements of free IAA, we observed that both *vas2-1* single and *vas2-1 sav3-1* double mutants possessed higher amounts of free IAA than WT under both Wc and shade conditions (Fig. 2e). These analytical measurements are consistent with the ability of *vas2* to suppress *sav3* short hypocotyls. In sharp contrast, the IAA-Glu levels in

both *vas2-1* single and *vas2-1 sav3-1* double mutants were about 20% of that of WT (Fig. 2g), which is consistent with the *in vitro* VAS2–GH3.17 enzyme assays showing Glu as the most efficient co-substrate for VAS2–GH3.17 catalysed IAA conjugation reactions (Fig. 1e). Under the conditions tested, it appears that the remaining seven VAS2–GH3.17 homologues cannot fully complement the physiological function of VAS2–GH3.17. Notably, IAA-Asp levels in *vas2* mutants were higher than the levels measured in WT plants (Fig. 2h). Elevated IAA-Asp levels in vas2 mutants may be a metabolic feedback response to the high levels of free IAA and catalysed *in vivo* by VAS2–GH3.17 homologues, including GH3.2, GH3.3, GH3.4 and GH3.5. All four IAA-amido synthetases have been shown to conjugate IAA to Asp (refs [15,16]). In contrast, VAS2–GH3.17 does not efficiently conjugate IAA to Asp (Fig. 1e).

Notably, the levels of IAA biosynthetic precursors and intermediates including anthranilate (ANT), L-Trp, and 3-IPA also increased as a result of *vas2* mutations (Fig. 2a–d), indicating that VAS2 activity feeds back on the auxin biosynthetic pathway to modulate IAA precursor pools. This is unexpected since one would reasonably posit that other free IAA catabolic pathways (for example, forming IAA–ester conjugates with sugar moieties, and conversion of IAA to indole-3-butyric acid (IBA)) would act to offset the free IAA accumulation of *vas2* mutations[18,23,24,27]. This argues that VAS2–GH3.17 plays a major role in modulating free IAA levels in *Arabidopsis* shoots.

VAS2–GH3.17 RNA accumulates to high levels in hypocotyls and its expression is downregulated by shade

We examined the expression pattern of *VAS2–GH3.17* using its promoter to drive the β-glucuronidase (GUS) reporter (*pVAS2::GUS*). *VAS2–GH3.17* is expressed weakly in the tips of cotyledons and new leaves, but strongly in roots and hypocotyls (Supplementary Fig. 3a–f). Notably, *VAS2–GH3.17* expression in hypocotyls declined modestly after 1 h of shade treatment, and more appreciably after 24 h in the shade (Supplementary Fig. 3g–i). Decreased *VAS2–GH3.17* expression in response to shade is likely to contribute to the rapid shade-triggered accumulation of free IAA in hypocotyls required for accelerated elongation.

vas2, unlike *vas1*, has longer hypocotyls in response to shade even when auxin transport from cotyledons is inhibited

To address whether the *vas2* phenotype depended on auxin transport from cotyledons to hypocotyls, we treated *Arabidopsis* seedlings with the auxin transport inhibitor 1-*N*-naphthylphthalamic acid (NPA) that efficiently curtails free IAA in cotyledons from moving to hypocotyls, fully inhibiting shade-stimulated hypocotyl elongation[4,8]. As reported previously, NPA fully suppressed the shade-induced hypocotyl elongation of WT (Fig. 3a,b). However, the same concentration of NPA used on WT seedlings only marginally affected the shade-induced hypocotyl length of *vas2* single and *vas2 sav3* double mutants (Fig. 3a,b). Other widely used auxin transport inhibitors such as 2-[4-(diethylamino)]-2-hydroxybenzoyl benzoic acid (BUM) and 2,3,5-triiodobenzoic acid (TIBA) that inhibit auxin transport by distinct molecular mechanisms exhibited similar growth phenotypes (Supplementary Fig. 4)[28]. Thus, *vas2* single and *vas2 sav3* double mutants signal hypocotyl elongation by mechanisms largely independent of *de novo* auxin biosynthesis in cotyledons and transport

to hypocotyls in response to shade. Notably, the *vas2* mutation fully rescued the short hypocotyl phenotype of the cotyledon-to-hypocotyl auxin transport mutant *pin3-4* during SAS[8] (Fig. 3c,d).

We previously reported a *sav3* suppressor *vas1* that, like *vas2*, fully rescues the low auxin levels and short hypocotyls of *sav3* mutants under shade[13]. VAS1 encodes a Met aminotransferase that catalyses the conversion of 3-IPA and Met to Trp and 2-oxo-4-methylthiobutyric acid, respectively, thus dampening the amount of Trp destined for IAA via 3-IPA. Interestingly, in sharp contrast to the *vas2 sav3* double mutant, the *vas1 sav3* double mutant was sensitive to the inhibitory effects of NPA on shade-induced hypocotyl elongation (Fig. 3e). This observation is consistent with the proposed role of VAS1 to suppress elevation of the IAA pools in cotyledons and newly formed leaves[4,13]. The sharp differences between *vas2* and *vas1* with regard to their sensitivities to NPA-mediated hypocotyl growth inhibition further argue that free IAA accumulates in *vas2* mutant hypocotyls independent of newly synthesized auxin in cotyledons.

vas2 mutation has no effect on the responses of the cotyledon's angle and size of *sav3* mutants to treatment with NPA and shade in combination. In WT seedlings, cotyledons bent downward (Fig. 4a,b) and were dramatically reduced in size with NPA treatment and shade (Fig. 4c,d). This growth effect results from the accumulation of high levels of IAA in cotyledons stemming from local shade-triggered auxin biosynthesis concomitant with blockage of IAA transport from cotyledons to hypocotyls. In contrast, the *sav3* mutant's cotyledons bent slightly upward with the same treatment (Fig. 4a,b). Finally, the cotyledon size of the *sav3* mutant was only slightly decreased (Fig. 4c,d). The IAA biosynthetic defect of the *sav3* mutant is likely to account for the insensitivity of the *sav3* mutant's cotyledons to NPA and shade treatment. Interestingly, the *vas2-1 sav3-1* double mutant behaved similarly to the *sav3-1* single mutant with NPA and shade treatment (Fig. 4). Collectively, these observations support the hypothesis that VAS2–GH3.17 functions principally in the hypocotyl where *VAS2–GH3.17* is strongly expressed (Supplementary Fig. 3a,b), to modulate seedling responses to shade.

Shade-induced *DR5::GUS* accumulation and epidermal localization in the hypocotyl of WT, but not of *vas2*, repressed by NPA

To deduce the auxin distribution in the hypocotyls of *vas2* mutants, we introduced the widely used auxin responsive reporter *DR5::GUS* into *vas2-1* single and *vas2-1 sav3-1* double mutants. *DR5::GUS* expression in *vas2-1* single and *vas2-1 sav3-1* double mutants was stronger than that in WT under both Wc and shade conditions (Fig. 5). Shade treatment significantly increased *DR5::GUS* expression in the hypocotyls of WT, but was completely abrogated by NPA treatment (Fig. 5 and Supplementary Fig. 5). These comparative observations are consistent with the inhibitory effects of NPA on shade-activated hypocotyl elongation of WT (refs [4,8]). In sharp contrast, *vas2* mutants under shade and treated with the same concentration of NPA as WT exhibited strong *DR5::GUS* expression in their hypocotyls (Fig. 5 and Supplementary Fig. 5). Furthermore, the *vas2* mutants under shade exhibited strong *DR5::GUS* expression in the epidermal cells of hypocotyls in the presence or absence of NPA (Fig. 5).

On the basis of the *DR5::GUS* expression patterns and intensities before and after shade treatments, we posit that shade-induced hypocotyl elongation of the *vas2-1 sav3-1* double mutant is partly due to shade-stimulated auxin transport from the hypocotyl's vasculature to its epidermal cells. However, we cannot fully rule out the possibility that the enhanced *DR5::GUS* intensity in the epidermal cells may be in part because more auxin is synthesized there as a result of accumulation of a higher amount of precursors in the *vas2* mutant. Notably, the shade-induced hypocotyl elongation of the *vas2-1* single mutant that is more pronounced than that of WT and the *vas2-1 sav3-1* double mutant is likely to be because of both shade-triggered *de novo* IAA biosynthesis through SAV3 and shade-stimulated auxin transport from the hypocotyl vasculature to its epidermis. The loss of IAA conjugation to Glu in *vas2* mutant hypocotyls results in elevated concentrations of free IAA, attendant activation of transport of IAA from the vasculature to the epidermal layer of cells, and the resultant insensitivity of *vas2* hypocotyl elongation to NPA inhibition.

VAS2–GH3.17 regulates high temperature-induced hypocotyl elongation

SAV3-mediated IAA biosynthesis is also required for high temperature-induced hypocotyl elongation, and the *sav3* mutant is impaired in high temperature-triggered hypocotyl elongation due to its IAA biosynthetic defect[4,6,10]. Interestingly, the *vas2* mutation fully rescues the short hypocotyl of the *sav3* mutant under high temperatures (Fig. 6a,b). In addition, *vas2* mutants, but not WT seedlings, when exposed to high temperatures, still elongate their hypocotyls in the presence of the auxin transport inhibitor NPA (Fig. 6a,b). Furthermore, high temperatures increase *DR5::GUS* expression in the hypocotyl of WT (Fig. 6c,e) whereas expression is abolished by NPA treatment (Fig. 6g). However, in the *vas2* mutant, NPA had no detectable effects on high temperature-stimulated *DR::GUS* expression in the hypocotyl and its lateral distribution to the outer layer of hypocotyl cells (Fig. 6d,f,h). *vas2* effects in seedlings at high temperature closely resemble phenotypes of *vas2* effects on seedlings subjected to shade (Fig. 5). These comparable growth outcomes strongly indicate that seedling responses to high temperature and shade use similar metabolic and signalling mechanisms to modulate hypocotyl elongation wherein VAS2–GH3.17 plays a pivotal role spatially and temporally.

Discussion

Genetic, biochemical and targeted metabolic analyses demonstrate that the IAA-amido synthetase, VAS2–GH3.17, spatially regulates the concentrations of free IAA spanning the hypocotyl by catalysing localized formation of inactive IAA-amido conjugates, which, in turn, feedback inhibit auxin biosynthesis. Through temporally and spatially activated VAS2–GH3.17 catalysis, VAS2–GH3.17 functions as a key modulator of auxin metabolism and rapid auxin spatial redistribution in response to environmental changes. In particular, VAS2–GH3.17's metabolic activity in the hypocotyl dictates the timing and magnitude of hypocotyl elongation in response to environmental cues, such as shade and high temperature (Supplementary Fig. 6).

Substantially reduced levels of IAA-Glu in *vas2* mutants may trigger the conversion of free IAA to storage forms of IAA conjugates (for example, methyl-IAA, IAA-glucose, etc.)[24]

rather than metabolites destined for degradation. These storage forms can lead to the mobilization and release of active IAA under particular environmental conditions such as shade to signal rapid elongation of hypocotyls (Supplementary Fig. 6). This may explain why *vas2 sav3* double mutants have increased free IAA levels and elongated hypocotyls in response to shade, even when shade-triggered new auxin biosynthesis is largely impaired in *sav3* single mutants.

The levels of IAA, IAA biosynthetic precursors, for example 3-IPA, and some IAA metabolites are significantly perturbed as a result of the *vas2* mutation with the exception of oxIAA (Fig. 2f). These results argue that conjugation of free IAA to amino acids (mainly Glu) by VAS2–GH3.17, rather than oxidation of IAA, plays a critical role in maintaining IAA homeostasis in *Arabidopsis* shoots. This metabolic trait in shoots stands in stark contrast to the role that oxIAA plays in regulating auxin homeostasis in *Arabidopsis* roots[29]. Thus, distinct organs may use disparate catabolic pathways for fine-tuning the concentration and location of active IAA.

GH3 proteins exist throughout the green plant lineage including the moss *Physcomitrella patens*, and play critical roles in plant interactions with biotic and abiotic stressors by regulating the homeostasis of phytohormones such as salicylic acid (SA), jasmonic acid (JA) and auxin[30–34]. For instance, the two GH3 genes in *P. patens* are critical for auxin homeostasis under unfavourable environments such as high temperature and darkness[35]. However, it is important to note that GH3.12–PBS3–GDG1 may not directly metabolize SA because *GH3.12* knockout mutant accumulates less total SA than WT (ref. [36]). Another consideration is that GH3.10–DFL2, a member of group I GH3 genes in *Arabidopsis* whose proposed function is to conjugate JA to amino acids, modulates hypocotyl elongation in response to red light, although its specific biochemical function remains elusive[37]. Besides VAS2–GH3.17, *Arabidopsis* genome encodes seven additional IAA-amido synthetases[15,19]. *In vitro*, these enzymes all catalyse, with varying levels of substrate diversity, the conjugation of free IAA to amino acids; for instance, GH3.2, GH3.3, GH3.4, GH3.5 and GH3.6 can all link free IAA to Asp, Met, Tyr and Trp[15]. Overexpression of GH3.2, GH3.5 or GH3.6–DFL1 causes dwarf plants including short hypocotyls, which has been attributed to attenuation of active IAA levels[23,38]. Possibly due to catalytic promiscuity and the resulting functional complementation by other members of the GH family, single knockout mutants of GH3.1, GH3.2, GH3.5, GH3.9 or GH3.17 appear normal with only modest insensitivity to the inhibitory effects of external IAA application on primary root elongation[15]. Interestingly, unlike mutations in VAS2–GH3.17, loss of function of GH3.9, a close homologue of VAS2, does not rescue the short hypocotyl of *sav3* mutant (Fig. 1d). This lack of complementation indicates that these IAA-amido synthetases may have distinct biochemical and biological functions that act together in a complex manner to fine-tune active IAA levels and concentration gradients required for temporal and spatial regulation of plant growth and development in response to diverse environments. This is indispensable for plant survival and fitness since plants perform and propagate poorly in the presence of too little or too much auxin[23].

Although the mechanisms by which shade and high temperature modulate the transcriptional activities of PIFs (phytochrome interacting factors) may be different, generally speaking,

both conditions elevate the Trp-dependent auxin biosynthetic pathway in cotyledons by rapidly upregulating the expression of some members of the *YUC* flavin monooxygenase family through PIFs (refs [3,5,7]). Our parallel studies on the responses of *vas2* mutants to shade and high temperature, either in the *sav3* mutant background or in the presence of NPA, reveal that plants use conserved metabolic fine-tuning mechanisms mainly through VAS2–GH3.17 to modulate auxin homeostasis and activity directly in the hypocotyls. The existence of convergent metabolic regulatory points in cotyledons through PIF transcriptional regulation of *YUC* flavin monooxygenases and in hypocotyls through VAS2 is likely to facilitate the rapid and complex responses of plant tissues to fluctuating environments.

A number of small molecule plant hormones regulate growth and development in response to environment changes[39,40]. The amount of auxin in a given cell—a combination of biosynthesis, storage, turnover and transport often dictates the magnitude, locale and timing of tissue- and organ-specific signalling pathways[41]. Recent studies have demonstrated that auxin transport coupled to auxin biosynthesis play critical roles in establishing the timing and orientation of auxin maxima that regulate organogenesis[23,41–45]. Notably, most auxin in plants exists in chemically modified forms that lack signalling activity. Recent studies have revealed the surprising link between modified auxins including amino acid conjugates and endoplasmic reticulum-localized intracellular auxin carriers, including PIN5–PIN6–PIN8 and PIN-LIKES (PILS)2–PILS5 (refs [46,47]). How the IAA-amido synthetases that biosynthesize the amino acid conjugates, the IAA-amido hydrolases that release free and active auxins such as IAA and the auxin transporters that move auxins throughout the plant are regulated is still poorly understood. Understanding the mechanisms underlying the fine-tuning of auxin homeostasis and the temporal–spatial distribution of active auxins, such as IAA needed for optimal plant growth, development and environmental adaption, is essential for predictively modulating plant growth and development[18,23,24,26,27].

Finally, auxin coordinates other plant hormone activities in specific tissues and organsto regulate plant growth in response to environmental fluctuations. Our current studies have unravelled the unexpected capacity of IAA-amido synthetase VAS2–GH3.17 to modulate the homeostasis, turnover and spatial distribution of free IAA in *Arabidopsis* hypocotyls in response to environmental stimuli, including shade and high temperature. This implies that both temperature and light signals can be perceived and transduced specifically in hypocotyls. This notion is consistent with previous observations showing hypocotyls as sites for sensing and responding to the ambient light environments[48–50]. Why, then, do plants synthesize new auxin in cotyledons and transport it to hypocotyls? One possible explanation is that VAS2 depletes the concentration of free IAA in hypocotyls to increase the movement of free IAA from cotyledons used for signal capture. Alternatively, auxin synthesized and moved from cotyledons may act as a chemical signal that allows a plant to distinguish self-shading from competition with neighbouring plants.

Methods

Plant materials

The *sav3-1* mutant, *sav3-3* mutant and *vas1-2* mutant have been described before[4,13]. The T-DNA lines Salk_094646 (*vas2-2*), CS112245 (*gh3.9*) and CS9363 (*pin3-4*) mutant were

ordered from the *Arabidopsis* Biological Resource Center (ABRC). All the mutants were in the *A. thaliana* Col-0 background.

Plant growth conditions and quantitative hypocotyl measurement

Plant growth conditions and a protocol for screening of *sav3* mutant suppressors have been described before[13]. For shade treatments, *Arabidopsis* seeds were grown on 1/2 MS plates or 1/2 MS supplemented with the indicated concentrations of auxin transport inhibitor (NPA, BUM or TIBA) and maintained under Wc for 5 days. Some of the plants were then retained in Wc for another 4 days, and the others were transferred to shade for 4 days. For high temperature experiments, seedlings were grown on 1/2 MS plates in a 22 °C growth chamber for 5 days, then moved to a 29 °C growth chamber for 4 days. For each experiment, 40 seeds of each genotype were germinated on the plates for observing the seedling phenotype, and 15 seedlings were scanned for quantification of hypocotyl length, cotyledon area and cotyledon angle. All experiments were repeated at least three times with consistent results. For hypocotyl measurement, the seedlings were scanned using an HP Scanjet 8300 Professional Image Scanner, and images were analysed using the ImageJ software (http://rsbweb.nih.gov/ij/). Unless specifically noted, experiments conducted on 1/2 MS plates were maintained at 22 °C in a growth chamber under Wc.

VAS2 protein expression and enzyme activities assay

The pHis8–VAS2 construct was transformed into *Escherichia coli* BL21 (DE3) cells. The cells were grown at 37 °C in Terrific broth (Invitrogen) until $A_{600\ nm}$ reached ~ 1.0, and then VAS2 expression was induced overnight by addition of 0.5 mM IPTG (isopropyl-β-D-thiogalactoside). Cells were resuspended in lysis buffer (50 mM Tris-HCl (pH 8.0), 500 mM NaCl, 20 mM imidazole, 1% (vol/vol) Tween 20, 10% (vol/vol) glycerol and 20 mM 2-mercaptoethanol) and were lysed by sonication. Recombinant VAS2–GH3.17 protein was purified by passing the soluble lysates through a Ni^{2+}-nitrilotriacetic acid agarose column and eluted with lysis buffer supplemented with 250 mM imidazole (pH 8.0), followed by further purification by size exclusion chromatography on a Superdex 75 HR26/60 column. Finally, VAS2-containing fractions where combined, concentrated by ultrafiltration and stored in 12.5 mM Tris·HCl (pH 8.0), 50 mM NaCl and 2 mM DTT buffer for enzymatic assays.

IAA-amido synthetase activity of VAS2 was analysed using a HPLC mass spectrometer equipped with an Agilent Zorbax Eclipse XDB-C18 (4.6 × 150 mm, 5 μm particle size) reversed-phase column employing a gradient from 4.9% (v/v) acetonitrile in 0.1% (v/v) formic acid to 94.9% (v/v) acetonitrile in 0.1% formic acid at a flow rate of 0.5 ml min^{-1}. The IAA-amido synthetase assays contained 50 mM Tris-HCl (pH 8.0), 2 mM $MgCl_2$, 2 mM ATP, 1 mM DTT, 1 mM IAA and 5 mM of 20 different amino acids, respectively, and performed at 25 °C. Enzymatic activity was followed by monitoring the loss of the substrate, IAA. Enzyme activities were calculated after integration of the IAA peak and compared with an internal standard.

Quantification of IAA and its metabolites

For quantification of ANT, Trp, 3-IPA, free IAA, oxIAA, IAA-Glu and IAA-Asp, plants were grown under Wc for 5 days, then kept in Wc or transferred to simulated shade for 1 h. Aerial portions of the seedlings were collected for quantification of these metabolites as described previously[22].

Supplementary Material

Refer to Web version on PubMed Central for supplementary material.

Acknowledgments

We thank M. Geisler for the generous gift of BUM, and the *Arabidopsis* Biological Resource Center for mutant seeds. These studies were supported by US National Institutes of Health (NIH) grant 5R01GM52413 to J.C., the Swedish Governmental Agency for Innovation Systems (VINNOVA) and the Swedish Research Council (VR) to K.L. and O.N., the Ministry of Education, Youth and Sports of the Czech Republic (the National Program for Sustainability I No. LO1204) to O.N., the National Science Foundation under award nos EEC-0813570 and MCB-0645794 to J.P.N. and the Howard Hughes Medical Institute (Z.Z., J.P.N., J.C.).

References

1. Franklin KA. Shade avoidance. New Phytol. 2008; 179:930–944. [PubMed: 18537892]
2. Casal JJ. Shade avoidance. Arabidopsis Book. 2012; 10:e0157. [PubMed: 22582029]
3. Li L, et al. Linking photoreceptor excitation to changes in plant architecture. Genes Dev. 2012; 26:785–790. [PubMed: 22508725]
4. Tao Y, et al. Rapid synthesis of auxin via a new tryptophan-dependent pathway is required for shade avoidance in plants. Cell. 2008; 133:164–176. [PubMed: 18394996]
5. de Wit M, Lorrain S, Fankhauser C. Auxin-mediated plant architectural changes in response to shade and high temperature. Physiol Plant. 2014; 151:13–24. [PubMed: 24011166]
6. Stepanova AN, et al. TAA1-mediated auxin biosynthesis is essential for hormone crosstalk and plant development. Cell. 2008; 133:177–191. [PubMed: 18394997]
7. Sun J, Qi L, Li Y, Chu J, Li C. PIF4-mediated activation of YUCCA8 expression integrates temperature into the auxin pathway in regulating *Arabidopsis* hypocotyl growth. PLoS Genet. 2012; 8:e1002594. [PubMed: 22479194]
8. Keuskamp DH, Pollmann S, Voesenek LA, Peeters AJ, Pierik R. Auxin transport through PIN-FORMED 3 (PIN3) controls shade avoidance and fitness during competition. Proc Natl Acad Sci USA. 2010; 107:22740–22744. [PubMed: 21149713]
9. Franklin KA, et al. Phytochrome-interacting factor 4 (PIF4) regulates auxin biosynthesis at high temperature. Proc Natl Acad Sci USA. 2011; 108:20231–20235. [PubMed: 22123947]
10. Yamada M, Greenham K, Prigge MJ, Jensen PJ, Estelle M. The TRANSPORT INHIBITOR RESPONSE2 gene is required for auxin synthesis and diverse aspects of plant development. Plant Physiol. 2009; 151:168–179. [PubMed: 19625638]
11. Procko C, Crenshaw CM, Ljung K, Noel JP, Chory J. Cotyledon-generated auxin is required for shade-induced hypocotyl growth in *Brassica rapa*. Plant Physiol. 2014; 165:1285–1301. [PubMed: 24891610]
12. Petrasek J, Friml J. Auxin transport routes in plant development. Development. 2009; 136:2675–2688. [PubMed: 19633168]
13. Zheng Z, et al. Coordination of auxin and ethylene biosynthesis by the aminotransferase VAS1. Nature Chem Biol. 2013; 9:244–246. [PubMed: 23377040]
14. Hagen G, Kleinschmidt A, Guilfoyle T. Auxin-regulated gene expression in intact soybean hypocotyl and excised hypocotyl sections. Planta. 1984; 162:147–153. [PubMed: 24254049]
15. Staswick PE, et al. Characterization of an *Arabidopsis* enzyme family that conjugates amino acids to indole-3-acetic acid. Plant Cell. 2005; 17:616–627. [PubMed: 15659623]

16. Westfall CS, Herrmann J, Chen Q, Wang S, Jez JM. Modulating plant hormones by enzyme action: the GH3 family of acyl acid amido synthetases. Plant Signal Behav. 2010; 5:1607–1612. [PubMed: 21150301]
17. Ludwig-Muller J. Auxin conjugates: their role for plant development and in the evolution of land plants. J Exp Bot. 2011; 62:1757–1773. [PubMed: 21307383]
18. Korasick DA, Enders TA, Strader LC. Auxin biosynthesis and storage forms. J Exp Bot. 2013; 64:2541–2555. [PubMed: 23580748]
19. Morant M, et al. Metabolomic, transcriptional, hormonal, and signaling crosstalk in superroot2. Mol Plant. 2010; 3:192–211. [PubMed: 20008451]
20. Paponov IA, et al. Comprehensive transcriptome analysis of auxin responses in *Arabidopsis*. Mol Plant. 2008; 1:321–337. [PubMed: 19825543]
21. Terol J, Domingo C, Talon M. The GH3 family in plants: genome wide analysis in rice and evolutionary history based on EST analysis. Gene. 2006; 371:279–290. [PubMed: 16488558]
22. Novak O, et al. Tissue-specific profiling of the *Arabidopsis thaliana* auxin metabolome. Plant J. 2012; 72:523–536. [PubMed: 22725617]
23. Ljung K. Auxin metabolism and homeostasis during plant development. Development. 2013; 140:943–950. [PubMed: 23404103]
24. Woodward AW, Bartel B. Auxin: regulation, action, and interaction. Ann Bot. 2005; 95:707–735. [PubMed: 15749753]
25. Rampey RA, et al. A family of auxin-conjugate hydrolases that contributes to free indole-3-acetic acid levels during *Arabidopsis* germination. Plant Physiol. 2004; 135:978–988. [PubMed: 15155875]
26. LeClere S, Tellez R, Rampey RA, Matsuda SP, Bartel B. Characterization of a family of IAA-amino acid conjugate hydrolases from *Arabidopsis*. J Biol Chem. 2002; 277:20446–20452. [PubMed: 11923288]
27. Sauer M, Robert S, Kleine-Vehn J. Auxin: simply complicated. J Exp Bot. 2013; 64:2565–2577. [PubMed: 23669571]
28. Kim JY, et al. Identification of an ABCB/P-glycoprotein-specific inhibitor of auxin transport by chemical genomics. J Biol Chem. 2010; 285:23309–23317. [PubMed: 20472555]
29. Pencik A, et al. Regulation of auxin homeostasis and gradients in *Arabidopsis* roots through the formation of the indole-3-acetic acid catabolite 2-oxindole-3-acetic acid. Plant Cell. 2013; 25:3858–3870. [PubMed: 24163311]
30. Khan S, Stone JM. *Arabidopsis thaliana* GH3.9 influences primary root growth. Planta. 2007; 226:21–34. [PubMed: 17216483]
31. Westfall CS, et al. Structural basis for prereceptor modulation of plant hormones by GH3 proteins. Science. 2012; 336:1708–1711. [PubMed: 22628555]
32. Yuan H, et al. Genome-wide analysis of the GH3 family in apple (*Malus* × *domestica*). BMC Genomics. 2013; 14:297. [PubMed: 23638690]
33. Fu J, Yu H, Li X, Xiao J, Wang S. Rice GH3 gene family: regulators of growth and development. Plant Signal Behav. 2011; 6:570–574. [PubMed: 21447996]
34. Khan S, Stone JM. *Arabidopsis thaliana* GH3.9 in auxin and jasmonate cross talk. Plant Signal Behav. 2007; 2:483–485. [PubMed: 19704592]
35. Mittag J, Gabrielyan A, Ludwig-Muller J. Knockout of GH3 genes in the moss *Physcomitrella patens* leads to increased IAA levels at elevated temperature and in darkness. Plant Physiol Biochem. 2015; 97:339–349. [PubMed: 26520677]
36. Jagadeeswaran G, et al. Arabidopsis GH3-LIKE DEFENSE GENE 1 is required for accumulation of salicylic acid, activation of defense responses and resistance to *Pseudomonas syringae*. Plant J. 2007; 51:234–246. [PubMed: 17521413]
37. Takase T, Nakazawa M, Ishikawa A, Manabe K, Matsui M. DFL2, a new member of the *Arabidopsis* GH3 gene family, is involved in red light-specific hypocotyl elongation. Plant Cell Physiol. 2003; 44:1071–1080. [PubMed: 14581632]

38. Nakazawa M, et al. DFL1, an auxin-responsive GH3 gene homologue, negatively regulates shoot cell elongation and lateral root formation, and positively regulates the light response of hypocotyl length. Plant J. 2001; 25:213–221. [PubMed: 11169197]
39. Santner A, Calderon-Villalobos LI, Estelle M. Plant hormones are versatile chemical regulators of plant growth. Nature Chem Biol. 2009; 5:301–307. [PubMed: 19377456]
40. Nemhauser JL, Hong F, Chory J. Different plant hormones regulate similar processes through largely nonoverlapping transcriptional responses. Cell. 2006; 126:467–475. [PubMed: 16901781]
41. Zhao Y. Auxin biosynthesis. Arabidopsis Book. 2014; 12:e0173. [PubMed: 24955076]
42. van Berkel K, de Boer RJ, Scheres B, ten Tusscher K. Polar auxin transport: models and mechanisms. Development. 2013; 140:2253–2268. [PubMed: 23674599]
43. Blilou I, et al. The PIN auxin efflux facilitator network controls growth and patterning in *Arabidopsis* roots. Nature. 2005; 433:39–44. [PubMed: 15635403]
44. Grieneisen VA, Xu J, Maree AF, Hogeweg P, Scheres B. Auxin transport is sufficient to generate a maximum and gradient guiding root growth. Nature. 2007; 449:1008–1013. [PubMed: 17960234]
45. Pinon V, Prasad K, Grigg SP, Sanchez-Perez GF, Scheres B. Local auxin biosynthesis regulation by PLETHORA transcription factors controls phyllotaxis in *Arabidopsis*. Proc Natl Acad Sci USA. 2013; 110:1107–1112. [PubMed: 23277580]
46. Mravec J, et al. Subcellular homeostasis of phytohormone auxin is mediated by the ER-localized PIN5 transporter. Nature. 2009; 459:1136–1140. [PubMed: 19506555]
47. Barbez E, et al. A novel putative auxin carrier family regulates intracellular auxin homeostasis in plants. Nature. 2012; 485:119–122. [PubMed: 22504182]
48. Morgan DC, O'Brien T, Smith H. Rapid photomodulation of stem extension in light-grown *Sinapis alba* L.: studies on kinetics, site of perception and photoreceptor. Planta. 1980; 150:95–101. [PubMed: 24306582]
49. Preuten T, Hohm T, Bergmann S, Fankhauser C. Defining the site of light perception and initiation of phototropism in *Arabidopsis*. Curr Biol. 2013; 23:1934–1938. [PubMed: 24076239]
50. Yamamoto Y, et al. Quality control of PSII: behavior of PSII in the highly crowded grana thylakoids under excessive light. Plant Cell Physiol. 2014; 55:1206–1215. [PubMed: 24610582]

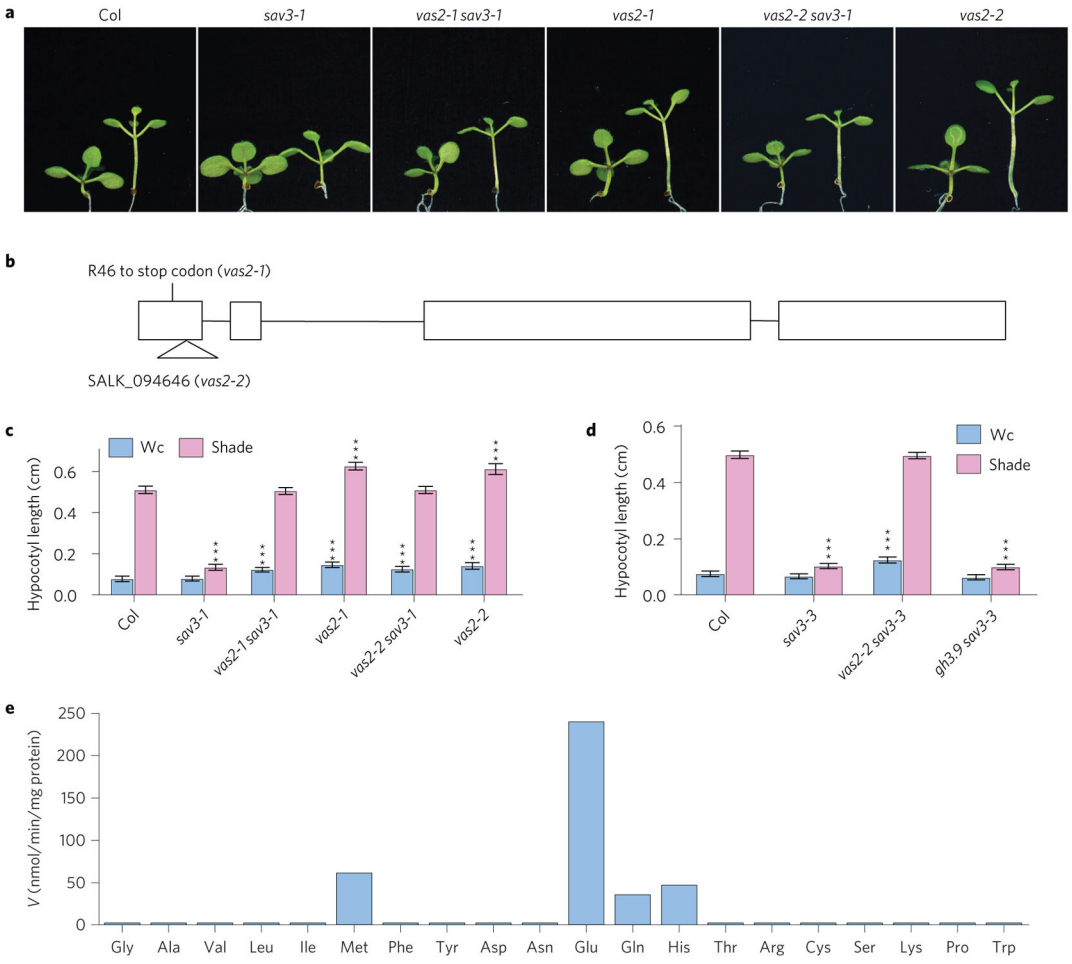

Figure 1. Identification of the *VAS2* gene

a, Representative plants of Col WT, *sav3* mutants and *vas2* mutants. Plants were grown on 1/2 MS plates and kept under Wc for 5 days, and then maintained in Wc for 4 days (plant on the left of each panel) or transferred to shade for 4 days (plant on the right of each panel). **b**, Diagram of the VAS2 genomic DNA sequence, with exons indicated by boxes. Mutation of *vas2-1* and the SALK T-DNA line *vas2-2* are shown. **c**, Quantification of hypocotyl length of plants grown under similar conditions as described above. **d**, *vas2-2*, but not *gh3.9*, can suppress the short hypocotyl of the *sav3-3* mutant under shade. In **c**,**d** the results are shown as mean ± s.e.m. ***$P < 0.001$ (two-tailed Student's *t*-test). The comparisons are between WT plants and mutant plants under the same growth conditions and the same treatment. **e**, Glu is the most efficient co-substrate of IAA-amido synthetase VAS2. VAS2 protein was expressed in *E. coli*, purified to homogeneity and assayed for conjugation activities using free IAA and the 20 natural amino acids, respectively. *V*, velocity.

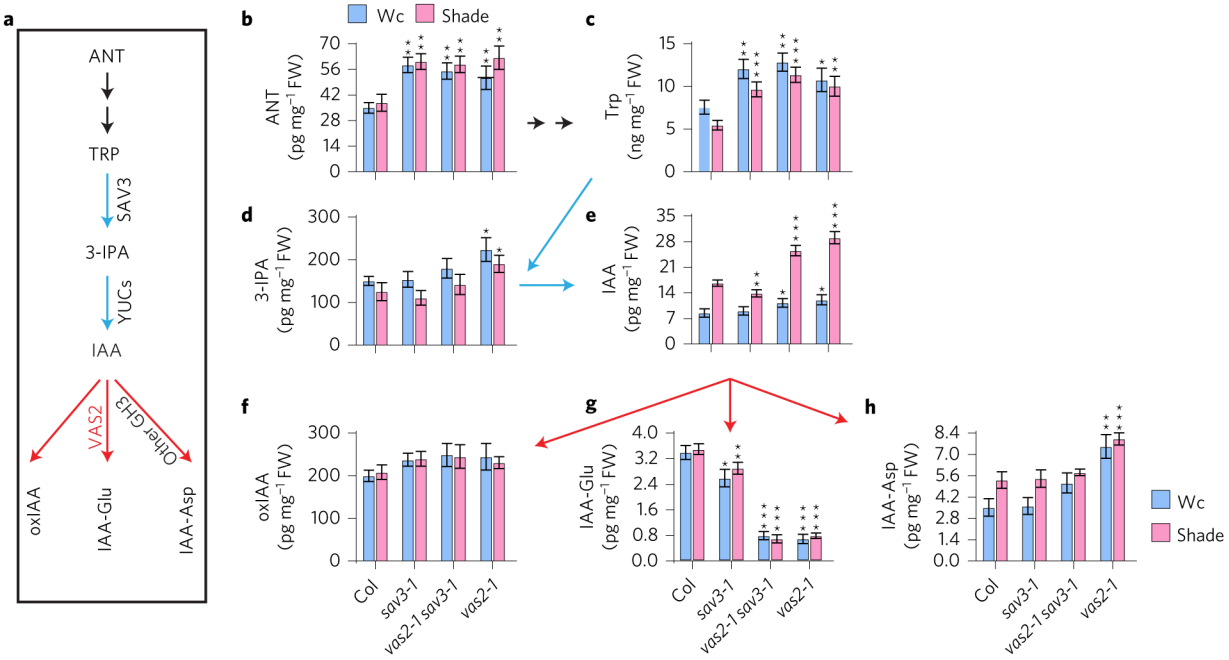

Figure 2. *vas2* mutant accumulates more free IAA and IAA biosynthetic precursors, but less of amino acid conjugate IAA-Glu

a, Major Trp-dependent IAA biosynthetic and catabolic/conjugating pathways in *A. thaliana*. ANT, anthranilate; Trp, tryptophan; 3-IPA, indole-3-pyruvic acid; IAA, indole-3-acetic acid; oxIAA, 2-oxoindole-3-acetic acid; IAA-Glu, IAA-glutamate; Other GH3, seven additional GH3 IAA-amido synthetases that can conjugate IAA to various amino acids including Asp *in vitro*. **b**, *vas2* mutants accumulate larger quantities of ANT. **c**, *vas2* mutants contain elevated amounts of Trp. **d**, *vas2* mutants possess larger amounts of 3-IPA. **e**, *vas2* mutants amass increased quantities of free IAA. **f**, *vas2* mutants accumulate similar concentrations of oxIAA as WT plants. **g**, *vas2* mutants possess smaller amounts of IAA-Glu. **h**, *vas2* mutants possess larger amounts of IAA-Asp. All results are shown as mean ± s.e.m. $*P < 0.05$, $**P < 0.01$ and $***P < 0.001$ (two-tailed Student's *t*-test). Comparisons are established between WT plants and mutant plants cultivated under the identical growth conditions and same treatments.

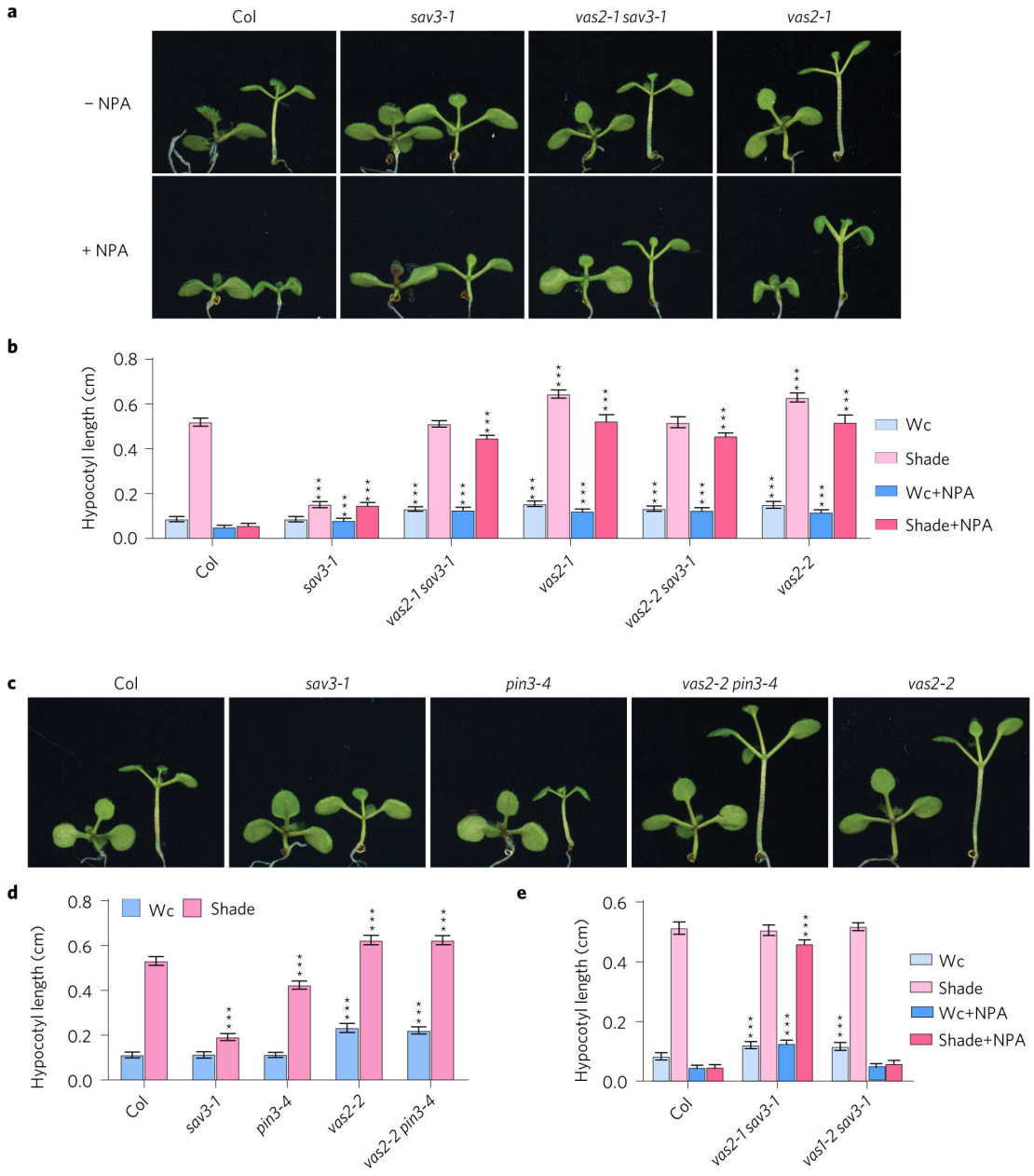

Figure 3. Shade-induced hypocotyl elongation of *vas2*, but not *vas1*, is largely independent of auxin transport from cotyledons to hypocotyls

a, Representative plants of WT, *sav3-1* mutant, *vas2 sav3-1* double mutant and *vas2-1* mutant are shown. Plants were grown on 1/2 MS (−NPA) or 1/2 MS containing 4 μM NPA (+NPA) for 5 days, then maintained in Wc for 4 days (plant on the left of each panel) or transferred to shade for 4 days (plant on the right of each panel). **b**, Quantification of hypocotyl length. **c**, Representative plants of WT, *sav3* mutants, *pin3-4* mutants, *vas2* mutants and *vas2 pin3-4* double mutants are shown. Plants were grown in similar conditions to those described above without NPA treatment. **d**, Quantification of hypocotyl length. **e**, Shade-induced hypocotyl elongation of *vas1-2 sav3-1* double mutant is strongly inhibited by

NPA. In **b**,**d**,**e** the results are shown as mean ± s.e.m. ***$P < 0.001$ (two-tailed Student's *t*-test). Comparisons are made between WT plants and mutants prepared using the same growth conditions and the same treatments.

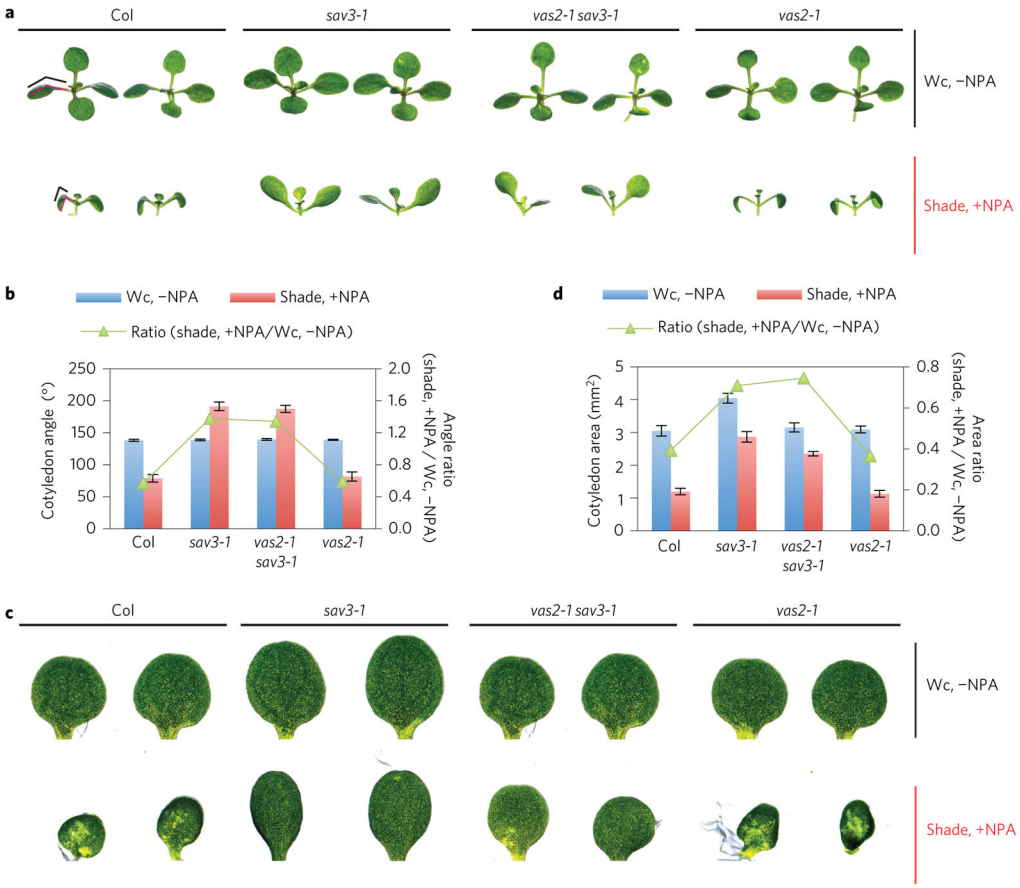

Figure 4. *vas2* mutation has no effect on the responses of the cotyledon's angle and size of the *sav3* mutant on treatment with a combination of NPA and shade

a, Representative plants of Col WT, *sav3-1* mutant, *vas2-1 sav3-1* double mutant and *vas2-1* mutant are shown. Plants were grown on 1/2 MS without NPA under Wc (Wc, −NPA) for 9 days or 1/2 MS containing 4 μM NPA for 5 days, then transferred to shade for 4 days (shade, +NPA). The cotyledon angle—the angle between the cotyledon and petiole—is denoted by red lines and further represented with black lines for clarification. **b**, Quantification of the cotyledon angle and the ratio of the cotyledon angle with shade and NPA treatment to that without shade treatment (shade, +NPA/Wc, −NPA). **c**, Representative cotyledons of Col WT, *sav3-1* mutant, *vas2 sav3-1* double mutant and *vas2-1* mutant are shown. Plant growth conditions are the same as described in Fig. 3a. **d**, Quantification of cotyledon size and the ratio of the cotyledon size with shade and NPA treatment to that without shade treatment (shade, +NPA/Wc, −NPA). Values are means ± s.e.m.

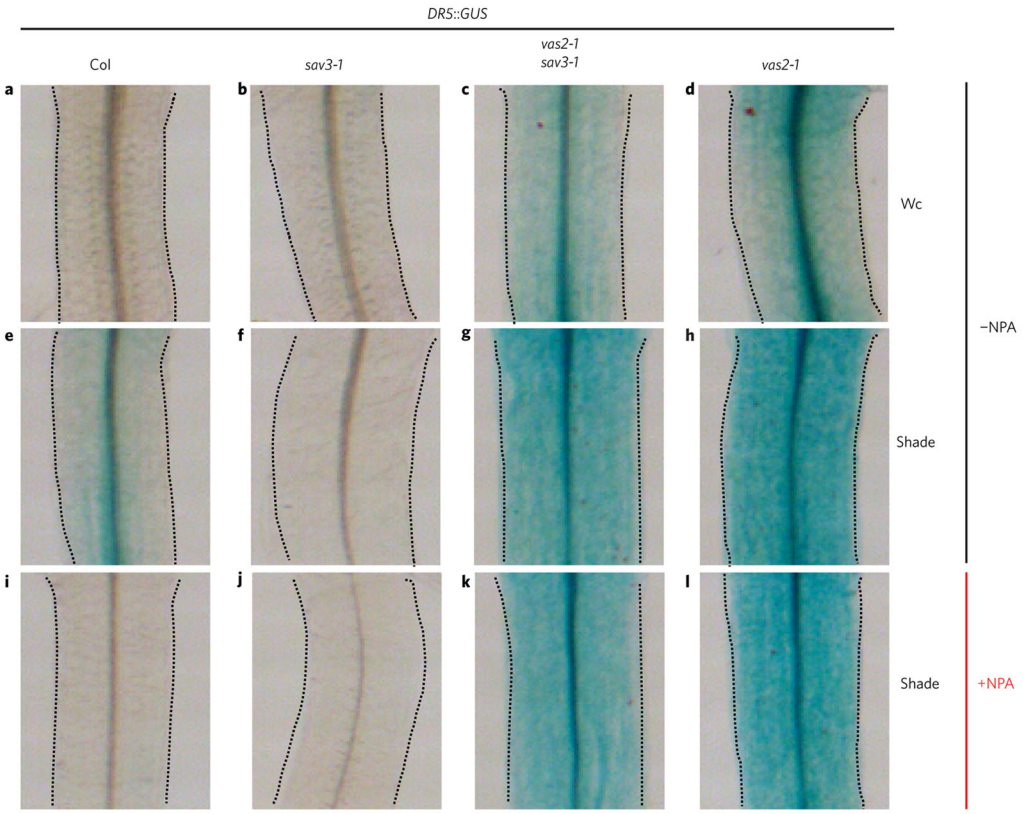

Figure 5. *DR5::GUS* intensity and distribution indicate that *vas2* mutant accumulates more free IAA, which is distributed to the epidermis of hypocotyl under shade regardless of NPA treatment

DR5::GUS was introduced into *sav3-1* mutant, *vas2-2* mutant and *vas2-2 sav3-1* double mutants by genetic cross. **a**–**h**, *vas2* mutants exhibit stronger *DR5::GUS* activities under both Wc and shade. Plants harbouring the *DR5::GUS* transgene were grown on 1/2 MS plates (−NPA) under Wc for 5 days, and then kept in Wc (**a**–**d**) or transferred to shade (**e**–**h**) for 4 days. **i**–**l**, NPA treatment inhibits *DR5::GUS* accumulation in the hypocotyl of WT plants, but not of *vas2* mutants. Plants harbouring the *DR5::GUS* transgene were grown on 1/2 MS plates supplemented with 4 μM NPA (+NPA) under Wc for 5 days, and then transferred to shade (**i**–**l**) for 4 days.

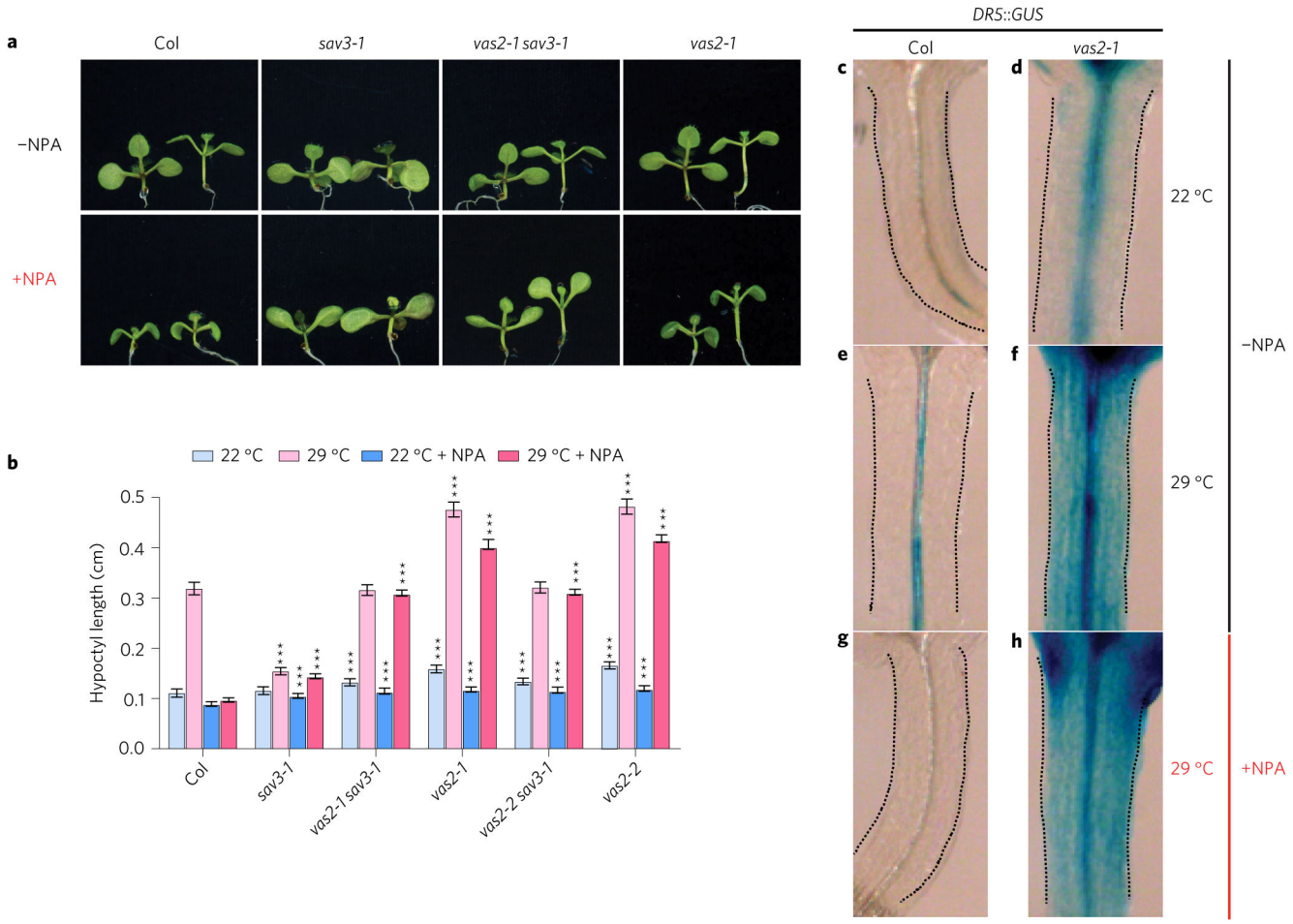

Figure 6. VAS2 regulates high temperature-induced hypocotyl elongation

a, Representative plants of WT, *sav3-1* mutant, *vas2 sav3-1* double mutant and *vas2-1* mutant are shown. Plants were grown on 1/2 MS (−NPA) or 1/2 MS containing 4 μM NPA (+NPA) for 5 days at 22 °C, then kept at 22 °C for 4 days (plants on the left of each panel) or transferred to 29 °C for 4 days (plants on the right of each panel). **b**, Quantification of hypocotyl length. The results are shown as mean ± s.e.m. ***$P < 0.001$ (two-tailed Student's *t*-test). Comparisons are made between WT plants and mutants prepared using the same growth conditions and the same treatments. **c**–**h**, *vas2* mutants exhibit stronger *DR5::GUS* expression under both 22 and 29 °C. Plants harbouring the *DR5::GUS* transgene were grown on 1/2 MS plates (−NPA) at 22 °C for 5 days, and then kept at 22 °C (**c**,**d**) or transferred to 29 °C (**e**–**h**) for 4 days. **g**–**h**, NPA treatment inhibits *DR5::GUS* accumulation in the hypocotyl of WT plants, but not of *vas2* mutants. Plants harbouring the *DR5::GUS* transgene were grown on 1/2 MS plates supplemented with 4 μM NPA (+NPA) at 22 °C for 5 days and then transferred to 29 °C for 4 days.